NanoNEXT

Research Article

DOI: 10.54392/nnxt2614

Enhanced Pseudocapacitive and Antimicrobial Behaviour of rGO-supported Sm^{3+}-Doped V_2O_5 Nanocomposites For High-Performance Energy Storage Applications

Senthil Kumar Nagarajan [a,*], S. Akshaya Devi [a], S. Aarthi [a], R. Swathi [a], S. Nagasundar [a], T. Kannan [a], M. Gowtham [b]

[a] Postgraduate and Research Department of Physics, Nanotechnology Lab, Kongunadu Arts and Science College, Coimbatore 641029, Tamil Nadu, India.

[b] Department of Physics, KGiSL Institute of Technology, Coimbatore, 641 035, Tamil Nadu, India

* Corresponding author Email: kumarsrkvphy@gmail.com

DOI: https://doi.org/10.54392/nnxt2614

Received: 07-12-2025; Revised: 13-03-2026; Accepted: 22-03-2026; Published: 28-03-2026

Abstract: The development of high-performance electrode materials remains a critical challenge in the advancement of electrochemical supercapacitors for next-generation energy storage systems. In the present work, reduced graphene oxide (rGO) supported vanadium pentoxide nanocomposites doped with samarium ions were successfully synthesized through a simple co-precipitation route followed by thermal treatment. The structural, morphological, and electrochemical properties of rGO/V_2O_5:Sm^{3+} nanocomposites with different samarium concentrations (0, 3, 5, and 7 wt. %) were systematically investigated. X-ray diffraction analysis confirmed the formation of orthorhombic crystalline V_2O_5 with good phase purity, while structural parameters revealed crystallite sizes in the nanometres range. Scanning electron microscopy and high-resolution transmission electron microscopy studies indicated the formation of rod-like nanostructures uniformly distributed over conductive graphene sheets. Energy dispersive spectroscopy verified the presence of vanadium, oxygen, samarium, and carbon elements in the prepared nanocomposites without detectable impurities. Electrochemical properties of the synthesized materials were evaluated using cyclic voltammetry measurements in a three-electrode system with 2 M KOH electrolyte. The obtained cyclic voltammograms revealed characteristic redox peaks associated with the pseudo capacitive behaviour of vanadium oxide. The specific capacitance values calculated from the CV curves demonstrated a strong dependence on samarium doping concentration. Among the prepared samples, the rGO/V_2O_5:Sm^{3+} nanocomposite containing 7 wt. % samarium exhibited the highest specific capacitance of approximately 386.70 F g^{-1}. The enhanced electrochemical performance is attributed to the synergistic interaction between the conductive graphene network, the nanorod morphology of V_2O_5, and the lattice modification induced by samarium incorporation. Furthermore, the electrode displayed good cycling stability during repeated electrochemical cycling. The antibacterial activity of rGO/Pure V_2O_5 and Sm^{3+}-doped rGO/V_2O_5 (7 wt. %) nanocomposites against Escherichia coli and Staphylococcus indicate that Sm^{3+} doping substantially improves the antibacterial performance. Thus, these findings suggest that rGO/V_2O_5:Sm^{3+} nanocomposites represent promising electrode materials for high-performance supercapacitor applications along with biomedical and cosmeceutical applications.

Keywords: Reduced Graphene Oxide, Vanadium Pentoxide, Samarium Doping, Nanocomposites, Electrochemical Supercapacitors, Electrochemical Energy Storage

1. Introduction

In recent decades, the rapid growth of electronic devices, electric vehicles, and renewable energy technologies has created an urgent demand for efficient and reliable energy storage systems [1]. Conventional energy storage devices such as batteries possess relatively high energy density but suffer from limited power density and slower charge–discharge rates. In contrast, electrochemical supercapacitors have emerged as promising alternatives because they offer high power density, rapid charge–discharge capability, long cycle life, and excellent reliability under repeated operation [2]. These advantages make supercapacitors attractive for applications in hybrid electric vehicles, portable electronic devices, and grid energy storage systems. The continuous development of advanced electrode materials is therefore essential for improving the performance of supercapacitors and enabling next-generation energy storage technologies [3].

Electrochemical capacitors are generally classified into two main categories based on their energy storage mechanisms: electric double layer capacitors (EDLCs) and pseudocapacitors [4]. EDLCs store energy through electrostatic charge accumulation at the interface between the electrode and electrolyte, typically using carbon-based materials such as activated carbon, carbon nanotubes, and graphene. In contrast, pseudocapacitors rely on fast and reversible Faradaic redox reactions occurring at or near the surface of transition metal oxide electrodes. Due to these redox processes, pseudo capacitors usually provide higher capacitance and energy density than EDLCs. Transition metal oxides such as RuO_2, MnO_2, NiO and V_2O_5 have therefore been extensively studied as promising pseudocapacitive materials for high-performance energy storage devices [5]. Among the various transition metal oxides, vanadium pentoxide (V_2O_5) has received considerable attention as an electrode material for supercapacitors due to its multiple oxidation states, layered crystal structure, high theoretical capacitance, and relatively low cost [6, 7]. The layered framework of V_2O_5 facilitates ion intercalation and de-intercalation processes during electrochemical reactions, which significantly enhances charge storage capability. Furthermore, vanadium-based oxides possess good chemical stability and environmental compatibility, making them suitable for large-scale energy storage applications. Recent studies have demonstrated that V_2O_5-based nanostructures exhibit improved electrochemical performance due to their increased surface area and shortened ion diffusion pathways [8].

However, despite these advantages, pristine V_2O_5 still suffers from some inherent limitations, including relatively poor electrical conductivity and slow electron transport kinetics [9]. These drawbacks can restrict its practical application as an efficient supercapacitor electrode. To overcome these limitations, researchers have explored various strategies such as nanostructure engineering, elemental doping, and hybridization with conductive carbon materials. In particular, combining V_2O_5 with carbon-based materials such as graphene or reduced graphene oxide (rGO) has proven to be an effective approach for improving electrical conductivity and enhancing overall electrochemical performance [10].

Reduced graphene oxide has attracted widespread interest in energy storage research because of its high surface area, good electrical conductivity, and excellent mechanical stability [11]. The presence of residual oxygen functional groups in rGO also facilitates strong interaction with metal oxide nanoparticles, enabling the formation of stable hybrid nanocomposites. When V_2O_5 nanostructures are anchored onto rGO sheets, the graphene network provides efficient electron transport pathways while simultaneously preventing particle aggregation [12]. This synergistic interaction significantly improves ion diffusion and charge transfer processes within the electrode material [13]. Another promising approach for improving the electrochemical performance of V_2O_5 is the incorporation of rare-earth dopants. Rare-earth ions can modify the electronic structure, enhance charge carrier mobility, and introduce additional active sites for redox reactions. Among various rare-earth elements, samarium (Sm^{3+}) has shown potential for improving the structural and electrochemical characteristics of transition metal oxide materials due to its unique electronic configuration and large ionic radius [14]. The introduction of Sm^{3+} ions into the V_2O_5 lattice can induce lattice distortion and increase defect density, which may enhance electrochemical activity and charge storage capability.

Besides the energy storage properties, semiconductor nanostructures are also being engineered for the direct antimicrobial activity to use them as potential for biomedical and cosmeceutical applications. The rGO-modified TiO_2 exhibited an enhanced antibacterial activity against E. hormaechei under UV–Visible light irradiation [15]. The enormous surface area of rGO also fosters strong physical contacts with bacterial cell walls, allowing for close contact between the nanocomposite and microbial cells. This contact can cause mechanical stress and direct membrane damage, leading in increased permeability, leaking of internal components, and ultimately cell death [16]. The presence of reduced graphene oxide (rGO) significantly enhances antibacterial performance by serving as an electron acceptor and transporter. This function helps to suppress charge recombination and consequently increases the production of reactive oxygen species (ROS), which are critical for antibacterial activity [17]. A number of researchers confirmed the effectiveness of charge carrier mobility and redox sites to prevent the bacterial growth and support of biomedicine [18-20].

Based on these considerations, the development of rGO-based V_2O_5 nanocomposites doped with rare-earth elements represents a promising strategy for designing high-performance supercapacitor electrodes. In the present study, rGO/V_2O_5 and Sm^{3+}-doped rGO/V_2O_5 nanocomposites with different samarium concentrations (0, 3, 5 and 7 wt. %) were

synthesized using a simple co-precipitation method. The structural, morphological, and compositional properties of the prepared nanocomposites were investigated using X-ray diffraction (XRD), scanning electron microscopy (SEM), high-resolution transmission electron microscopy (HR-TEM), and energy dispersive spectroscopy (EDS). Furthermore, the electrochemical behaviour of the synthesized nanocomposites was evaluated through cyclic voltammetry measurements to determine their potential application as electrode materials for advanced supercapacitor devices also, their antimicrobial properties were explored.

2. Experimental Section

2.1 Materials

All chemicals used in this investigation were of analytical grade and were used without further purification. Ammonium metavanadate (NH_4VO_3), samarium (III) nitrate hexahydrate ($Sm(NO_3)_3 \cdot 6H_2O$), concentrated hydrochloric acid (HCl), graphite powder, sodium nitrate ($NaNO_3$), potassium permanganate ($KMnO_4$), hydrogen peroxide (H_2O_2), ethanol, and de-ionized water were employed as starting materials for the synthesis of the nanocomposites. The chemicals were selected because of their high purity and compatibility with solution-based synthesis methods. Transition metal oxide nanostructures prepared through wet chemical routes often exhibit better crystallinity and compositional homogeneity when high-purity precursors are used. Solution-based chemical synthesis methods are widely adopted for preparing electrode materials for supercapacitors because they enable good control over particle morphology, crystallite size, and compositional tuning [21].

2.2 Preparation of Pure V_2O_5 and Sm^{3+} Doped V_2O_5

Vanadium pentoxide nanoparticles were synthesized through a simple co-precipitation technique, which is considered a reliable and scalable approach for producing metal oxide nanostructures with controlled morphology. In a typical synthesis procedure, ammonium metavanadate was dissolved in 30 mL of de-ionized water and magnetically stirred for approximately 30 minutes at room temperature to obtain a homogeneous precursor solution. A few drops of hydrochloric acid were then slowly added to the solution in order to initiate precipitation and to regulate the pH of the reaction medium. The mixture was continuously stirred for an additional 20 minutes, leading to the formation of a yellow precipitate corresponding to the vanadium oxide precursor.

The precipitated product was collected through filtration and thoroughly washed several times using ethanol and de-ionized water in order to remove any residual ions or unreacted precursor species. The washed material was subsequently dried at room temperature for 24 hours to eliminate moisture. Finally, the dried precursor was calcined at 600 °C for 5 hours in order to obtain crystalline vanadium pentoxide (V_2O_5). Thermal treatment during calcination promotes crystallization and removes residual organic or hydroxyl species, thereby improving the structural stability of the final material. Similar synthesis conditions have been widely reported for preparing crystalline V_2O_5 nanostructures suitable for electrochemical energy storage applications [22].

For the preparation of samarium-doped V_2O_5 samples, the same procedure was followed with the addition of samarium (III) nitrate hexahydrate as the dopant precursor. Different weight percentages of Sm^{3+} ions (3, 5, and 7 wt. %) were introduced into the precursor solution prior to precipitation. The rare-earth dopant ions become incorporated into the V_2O_5 lattice during the calcination process, which can modify the structural properties and electronic characteristics of the resulting oxide material. Rare earth doping is known to introduce lattice distortions and defect sites that enhance electrochemical activity in transition metal oxides [23].

2.3 Synthesis of rGO

Reduced graphene oxide was synthesized using the modified Hummers method, which is one of the most widely used chemical approaches for producing graphene-based materials on a large scale. In this method, graphite powder was oxidized in a strongly acidic medium in order to introduce oxygen-containing functional groups into the graphite structure, thereby facilitating exfoliation into graphene oxide sheets. Initially, a reaction beaker containing concentrated sulphuric acid was placed in an ice bath maintained at approximately 0 °C to control the reaction temperature. Graphite powder was gradually added into the acid solution under continuous stirring. Sodium nitrate was then introduced into the mixture, followed by the slow addition of potassium permanganate as the oxidizing agent. The oxidation process resulted in the formation of graphite oxide with abundant oxygen-containing functional groups such as hydroxyl, epoxy, and carboxyl groups.

After oxidation, de-ionized water was slowly added to the mixture, which caused the temperature to increase and promoted the exfoliation of graphite oxide layers. Hydrogen peroxide was then introduced dropwise to terminate the oxidation reaction and to reduce residual permanganate ions. The resulting product was filtered and washed repeatedly to remove acidic impurities. Finally, the material was subjected to thermal treatment at 300 °C for two hours, which reduced graphene oxide into reduced graphene oxide (rGO). The reduction process restores partial electrical conductivity by removing a significant fraction of oxygen functional groups and reconstructing the conjugated graphene network. Reduced graphene oxide has been widely used as a conductive matrix in nanocomposite electrode materials because of its excellent electrical conductivity and large surface area [24].

2.4 Synthesis of rGO/V2O5:Sm^{3+} Nanocomposites

The rGO/V_2O_5:Sm^{3+} nanocomposites were synthesized through a simple mixing and thermal treatment approach. In a typical preparation, 0.5 g of the synthesized V_2O_5 or Sm^{3+}-doped V_2O_5 powder was dispersed in 100 mL of de-ionized water. Subsequently, 0.1 g of reduced graphene oxide was added to the suspension. The mixture was magnetically stirred for approximately one hour at room temperature to ensure uniform dispersion of V_2O_5 nanoparticles over the graphene sheets. During this process, the oxide particles become anchored onto the surface of rGO due to electrostatic interactions and physical adsorption. After thorough mixing, the suspension was filtered and washed several times using ethanol and de-ionized water to remove loosely attached particles. The resulting composite material was then calcined at 400 °C for two hours to improve interfacial contact between V_2O_5 nanoparticles and the rGO matrix. The formation of such hybrid nanostructures enhances electron transport pathways and prevents particle agglomeration, thereby improving electrochemical performance in energy storage devices [25].

2.5 Material Characterization

The structural and morphological characteristics of the synthesized nanocomposites were investigated using several advanced characterization techniques. The crystal structure and phase purity of the prepared samples were examined using powder X-ray diffraction (XRD) analysis with Cu Kα radiation (λ = 0.15406 nm). XRD measurements were performed using a Shimadzu XRD-6000 diffractometer. The diffraction patterns obtained from XRD analysis provide valuable information regarding crystallinity, lattice parameters, and average crystallite size of the materials. Surface morphology and microstructural features of the nanocomposites were analysed using field emission scanning electron microscopy (FE-SEM, Hitachi SU-8000) operating at an accelerating voltage of 10 kV. High-resolution transmission electron microscopy (HR-TEM) using a JEOL JEM-2100 microscope was employed to further investigate particle morphology and crystallographic structure at the nanoscale level. Elemental composition and distribution within the nanocomposite samples were determined through energy dispersive X-ray spectroscopy (EDS) attached to the SEM instrument. These combined characterization techniques provide comprehensive information regarding the structural integrity and compositional uniformity of the synthesized materials.

2.6 Electrochemical Measurements

The electrochemical performance of the prepared rGO/V_2O_5:Sm^{3+} nanocomposites was evaluated using cyclic voltammetry (CV) measurements in a three-electrode configuration. A 2 M potassium hydroxide (KOH) aqueous solution was used as the electrolyte because of its high ionic conductivity and stability for alkaline electrochemical systems. The working electrode was prepared by dispersing 1 mg of the nanocomposite material in 1 mL of distilled water followed by ultrasonication for approximately 30 minutes to obtain a uniform suspension. A small volume (3 µL) of the dispersion was drop-cast onto the surface of a glassy carbon electrode (GCE) and allowed to dry at 60 °C under reduced pressure for one hour. To improve adhesion and mechanical stability of the electrode coating, a small quantity of Nafion solution (0.5 wt. % in ethanol) was applied over the deposited material and dried again at 30 °C for three hours. The electrochemical measurements were carried out using an electrochemical workstation with the modified GCE as the working electrode, a platinum wire as the counter electrode, and an Ag/AgCl electrode as the reference electrode. The specific capacitance of the electrode materials was calculated from the cyclic voltammetry curves using the standard electrochemical relation between current response, scan rate, and potential window. The electrochemical characteristics obtained from CV measurements provide important information about charge storage behaviour, redox

reactions, and ion transport processes occurring within the electrode material.

3. Result and Discussion

3.1 X-Ray Diffraction Analysis

The crystal structure and phase purity of the synthesized rGO/V_2O_5 and rGO/V_2O_5:Sm^{3+} nanocomposites were analysed using X-ray diffraction (XRD). The diffraction patterns confirm that the prepared materials possess a well-defined orthorhombic crystal structure corresponding to vanadium pentoxide. The observed diffraction peaks are in good agreement with the standard diffraction data of orthorhombic V_2O_5 (JCPDS card no. 72-0598), indicating the successful formation of the desired crystalline phase without any secondary impurity phases. The prominent diffraction peaks corresponding to the crystallographic planes (200), (010), (110), (101), (400), (011), (301), (020), (411), (600), (121), (002), (012), (421), (312), and (701) appear at diffraction angles around 15.5°, 20.5°, 21.9°, 26.5°, 31.2°, 32.5°, 34.4°, 41.4°, 45.6°, 47.4°, 49.0°, 51.3°, 55.8°, 59.2°, 61.2°, and 62.2°, respectively. The sharp and narrow diffraction peaks observed in the XRD patterns (Figure 1) indicate that the synthesized nanocomposites possess good crystallinity.

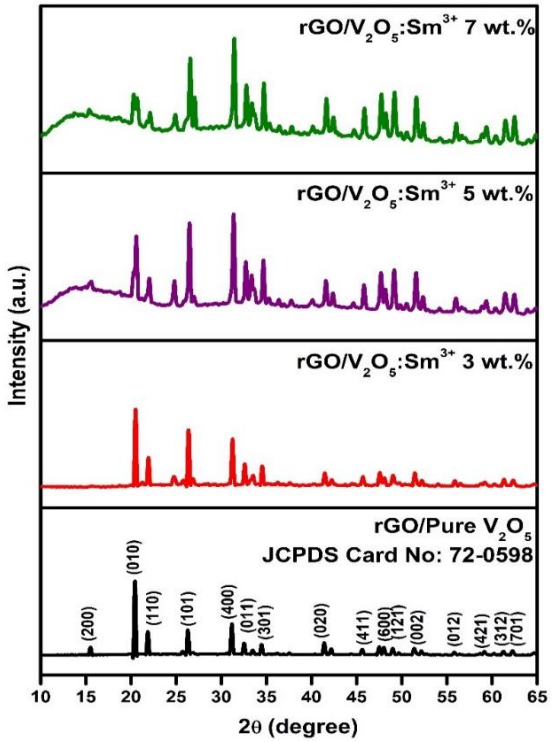

Figure 1. XRD Spectrum of rGO/V_2O_5:Sm^{3+} (0, 3, 5 and 7 wt. %) nanocomposites

The presence of reduced graphene oxide within the composite matrix does not significantly disturb the crystalline structure of V_2O_5, although slight variations in peak intensity are observed with increasing Sm^{3+} doping concentration. In particular, the intensity of the (200) diffraction peak gradually decreases after the incorporation of rGO and samarium ions, suggesting a modification in the lattice structure due to dopant incorporation and interaction with graphene sheets. Similar structural modifications have been reported in graphene-based transition metal oxide nanocomposites where lattice distortion occurs due to dopant substitution and interfacial interactions with carbon materials [26].

The crystallite size of the prepared samples was estimated using the Debye–Scherrer equation, which relates the broadening of diffraction peaks to the size of crystalline domains. The calculated average crystallite sizes of the rGO/V_2O_5:Sm^{3+} nanocomposites range from approximately 66 nm to 87 nm. The variation in crystallite size with increasing samarium content indicates that the dopant ions influence the nucleation and growth of V_2O_5 crystallites during the synthesis process. Rare-earth dopants are known to influence grain growth by altering lattice strain and defect density within the crystal structure.

In addition to crystallite size, other structural parameters such as microstrain and dislocation density were also determined from the XRD data. The calculated microstrain values fall within the range of approximately 0.00148 to 0.00172, indicating slight lattice distortion within the crystal structure. Dislocation density, which represents the number of lattice defects present in the crystal, varies with doping concentration and shows a tendency to decrease at higher dopant levels. These variations suggest that samarium incorporation modifies the internal lattice structure and may influence charge transport behaviour in the electrode material. Structural defects and lattice distortions often contribute to enhanced electrochemical activity by providing additional active sites for redox reactions and facilitating ion diffusion within the electrode material [27].

The lattice parameters calculated from the diffraction data also confirm slight structural changes in the orthorhombic lattice upon Sm^{3+} doping. These changes arise because the ionic radius of samarium differs from that of vanadium, resulting in lattice distortion when samarium ions partially substitute vanadium sites or occupy interstitial positions.

Table 1. Structural parameters of rGO/ V_2O_5:Sm^{3+} composites

Material	Average crystallite size (nm)	Average micro strain	Average dislocation density ×10^{14} (line/m^2)	Lattice parameters (Å)		
				a	b	c
rGO/Pure V_2O_5	87.3392	0.001587	2.1947	11.495	4.346	3.557
rGO/ V_2O_5:Sm^{3+} 3 wt.%	66.1847	0.001724	3.1017	11.447	4.331	3.555
rGO/ V_2O_5:Sm^{3+} 5 wt.%	80.9881	0.001488	1.8928	11.395	4.384	3.542
rGO/ V_2O_5:Sm^{3+} 7 wt.%	78.1193	0.001594	2.2011	11.374	4.382	3.544

Such structural modifications are often beneficial for electrochemical energy storage applications because they create additional pathways for ion transport and improve electrochemical kinetics. Table 1 lists the Structural parameters of rGO/ V_2O_5:Sm^{3+} composites. Overall, the XRD analysis confirms the successful synthesis of crystalline rGO/V_2O_5:Sm^{3+} nanocomposites with orthorhombic structure, good phase purity, and controlled crystallite size.

3.2 SEM and EDS Analysis

The surface morphology and microstructural characteristics of the synthesized nanocomposites were examined using scanning electron microscopy (SEM). The SEM images (Figure 2) reveal that the prepared rGO/V_2O_5:Sm^{3+} nanocomposites exhibit a rod-like nanostructured morphology with relatively uniform distribution. These nanorod structures appear to be loosely aggregated and distributed over the graphene sheets, forming a porous network structure. The presence of reduced graphene oxide within the composite matrix prevents excessive particle agglomeration and facilitates the formation of well-distributed nanostructures.

The formation of rod-like nanostructures is particularly advantageous for electrochemical applications because such morphologies provide a larger active surface area for electrolyte interaction. Increased surface area enables more electrochemically active sites for charge storage reactions, thereby improving the overall capacitance of the electrode material. Moreover, the porous arrangement of nanorods creates open pathways for electrolyte penetration, which facilitates efficient ion transport during electrochemical cycling. Previous studies have demonstrated that nanorod and nanowire structures of V_2O_5 provide improved electrochemical performance due to enhanced ion diffusion and increased electrode–electrolyte contact area [28].

Energy dispersive X-ray spectroscopy (EDS) analysis was conducted to verify the elemental composition of the synthesized nanocomposites. The EDS spectra (Figure 3) clearly confirm the presence of vanadium (V), oxygen (O), samarium (Sm), and carbon (C) elements in the prepared samples. The absence of additional peaks in the spectra indicates that no detectable impurities are present in the synthesized materials. Elemental mapping (Figure 4 a-b, Figure 5 a-b) further confirms the uniform distribution of these elements throughout the composite structure, suggesting successful integration of samarium dopants and graphene within the V_2O_5 matrix. The homogeneous distribution of carbon, vanadium, oxygen, and samarium elements plays an important role in improving electrochemical performance. Uniform dispersion of graphene sheets ensures effective electrical conductivity pathways, while the distributed metal oxide nanoparticles provide active sites for Faradaic reactions. Such synergistic interaction between graphene and metal oxide components has been widely reported to enhance charge storage capability in composite electrode materials [29].

3.3 HR-TEM Analysis

High-resolution transmission electron microscopy (HR-TEM) was employed to further investigate the microstructural features of the synthesized nanocomposites at the nanoscale level. The HR-TEM images (Figure 6a-d) clearly reveal the rod-like morphology of the rGO/V_2O_5:Sm^{3+} nanocomposites, which is consistent with the observations obtained from SEM analysis. The nanorods appear to be well dispersed on the surface of the reduced graphene oxide sheets, forming a hybrid nanostructure.

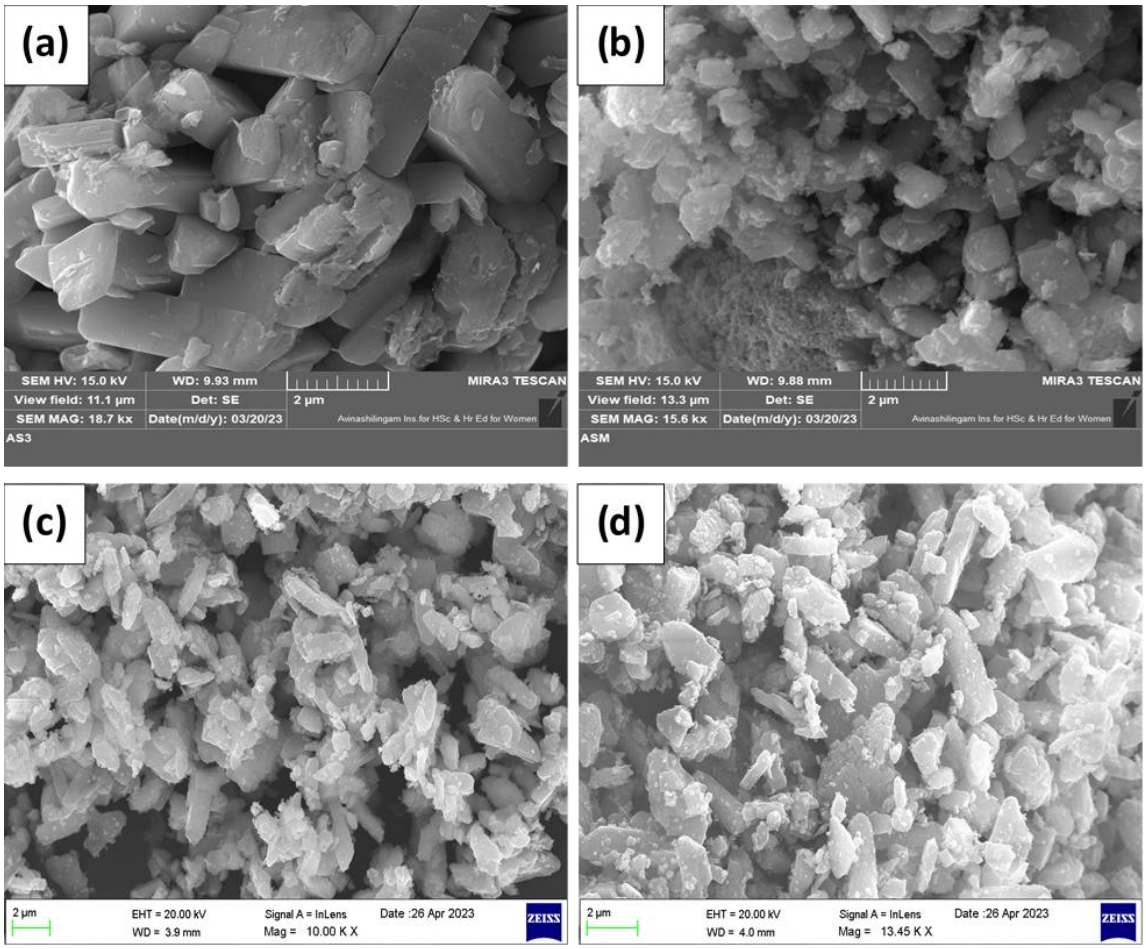

Figure 2. The surface morphology of rGO/V_2O_5:Sm^{3+} (0, 3, 5 and 7 wt. %) nanocomposites

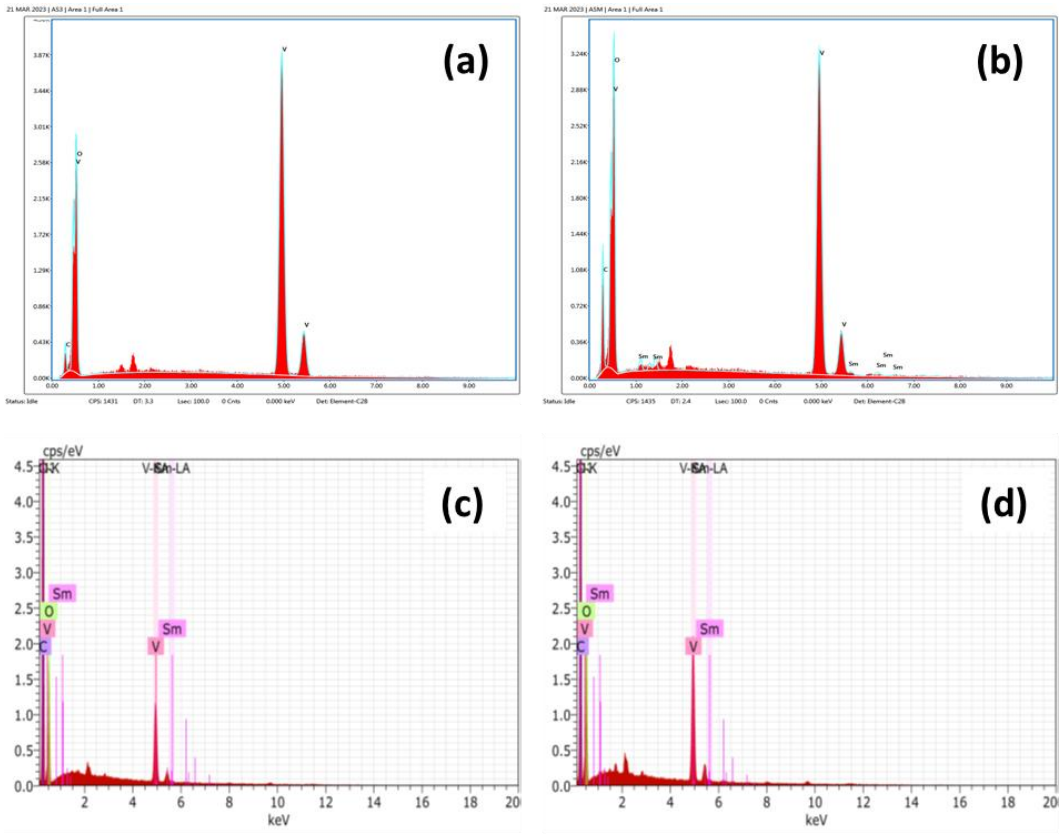

Figure 3. The surface morphology of rGO/V_2O_5:Sm^{3+} (0, 3, 5 and 7 wt. %) nanocomposites

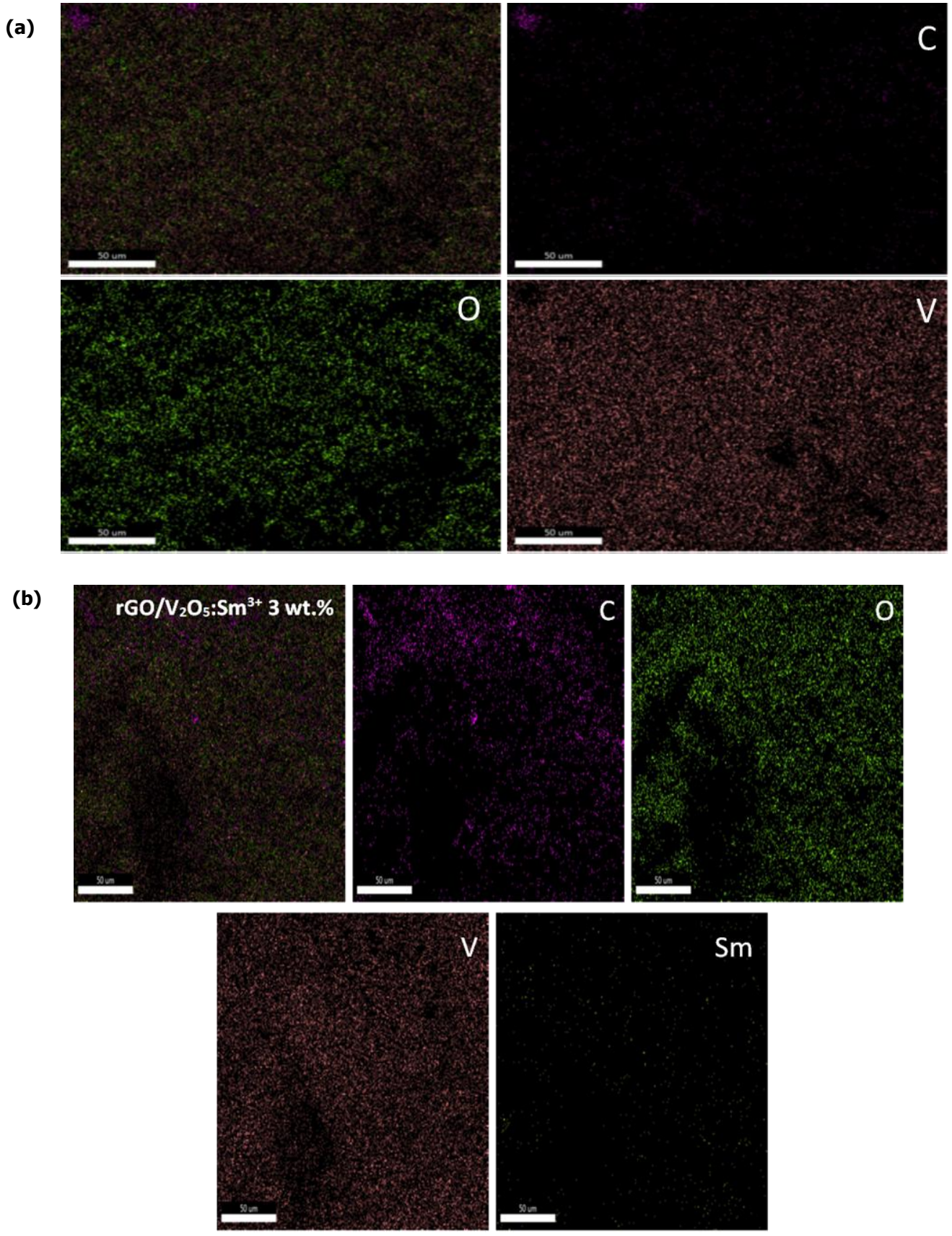

Figure 4 (a). Elemental Mapping of pure rGO/V_2O_5:Sm^{3+} (0 wt. %) nanocomposites, **(b).** Elemental Mapping of pure rGO/V_2O_5:Sm^{3+} (3 wt. %) nanocomposites

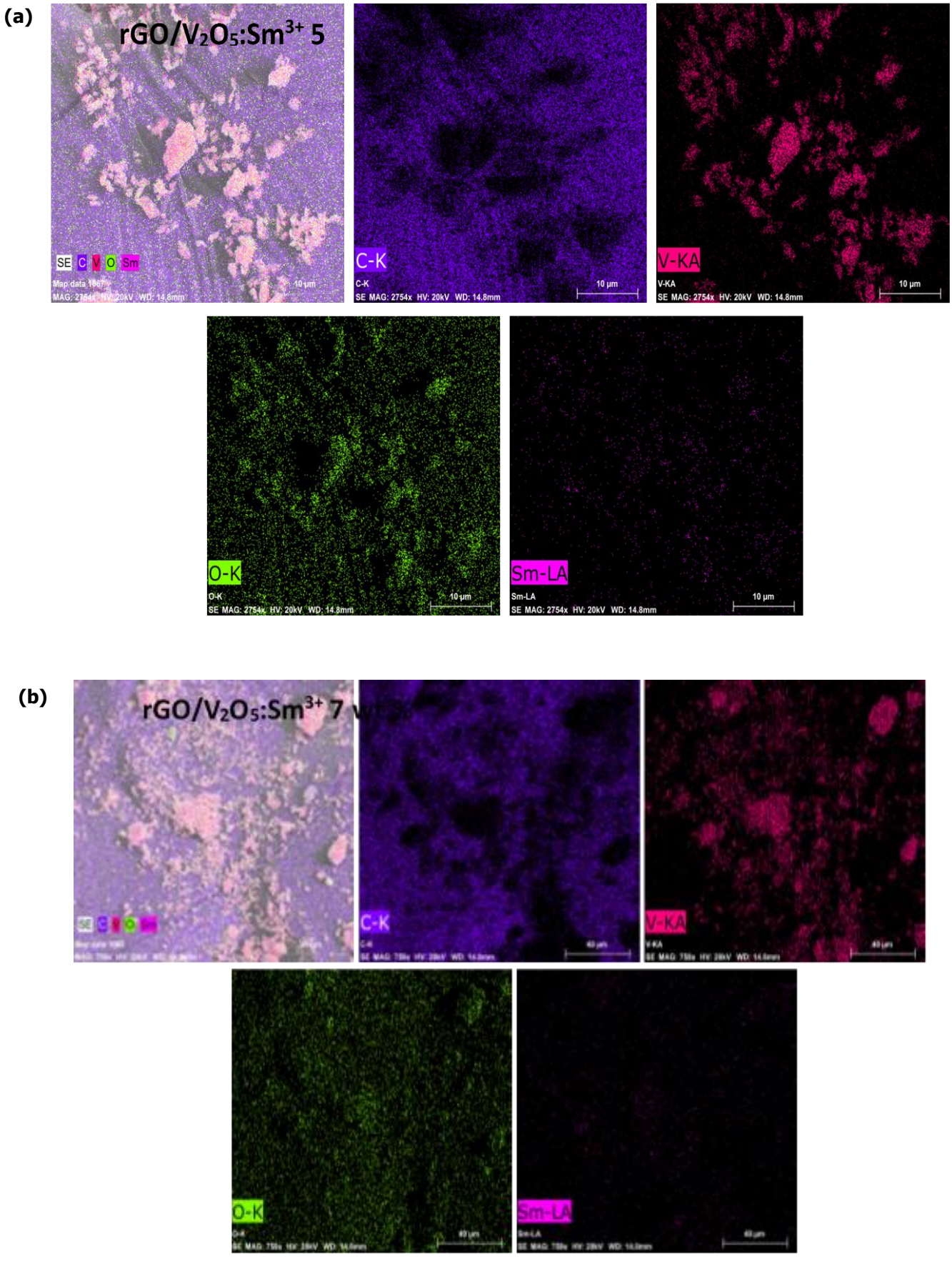

Figure 5 (a). Elemental Mapping of pure rGO/V2O5:Sm3+ (5 wt. %) nanocomposites, **(b).** Elemental Mapping of pure rGO/V2O5:Sm3+ (7 wt. %) nanocomposites

The intimate contact between V_2O_5 nanorods and graphene sheets is particularly beneficial for electrochemical applications. Graphene provides a conductive framework that facilitates rapid electron transport during electrochemical reactions, while the V_2O_5 nanorods serve as active pseudocapacitive materials responsible for charge storage.

This combination significantly enhances both electrical conductivity and electrochemical activity. The selected area electron diffraction (SAED) patterns (figure 6e-h) obtained from HR-TEM measurements show distinct diffraction rings and bright spots, indicating the polycrystalline nature of the synthesized nanocomposites. The presence of well-defined diffraction spots further confirms the high crystallinity of the prepared materials. Polycrystalline structures with nanoscale grains often exhibit improved electrochemical behaviour because grain boundaries can act as additional active sites for ion diffusion and redox reactions.

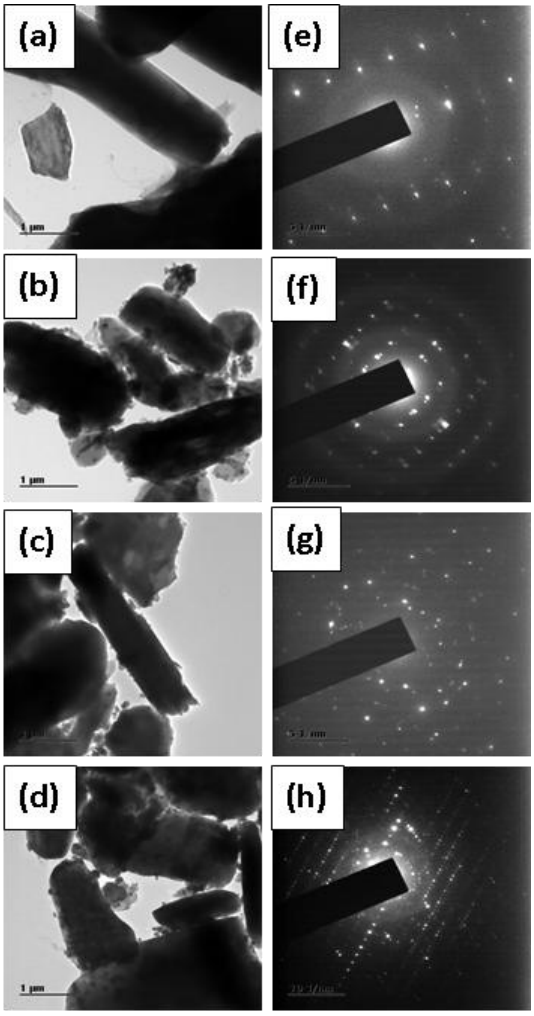

Figure 6. The TEM images (a – d) and SAED pattern (e – h) of rGO/V_2O_5:Sm^{3+} (0, 3, 5 and 7 wt. %) nanocomposites

3.4 Electrochemical Performance

The electrochemical performance of the rGO/V_2O_5:Sm^{3+} nanocomposite electrodes was evaluated using cyclic voltammetry (CV) in a three-electrode system with 2 M KOH aqueous electrolyte. The CV curves recorded at different scan rates ranging from 5 to 100 mV s^{-1} reveal the characteristic electrochemical behaviour of the electrode materials. The CV curves (Figure 7) exhibit distinct redox peaks, which clearly indicate the occurrence of Faradaic charge storage processes associated with the pseudocapacitive behaviour of the V_2O_5 electrode material. These redox peaks correspond to reversible oxidation and reduction reactions involving vanadium ions in different oxidation states. The presence of these peaks confirms that the charge storage mechanism of the synthesized nanocomposites is dominated by pseudocapacitance rather than purely electrostatic double-layer capacitance. Similar electrochemical behaviour has been widely reported for vanadium oxide-based supercapacitor electrodes [30].

The specific capacitance values calculated from the CV curves show a clear dependence on the samarium doping concentration. The calculated capacitance values for rGO/V_2O_5:Sm^{3+} (0, 3, 5, and 7 wt. %) nanocomposites are approximately 169.65, 194.90, 204.49, and 386.70 F g^{-1}, respectively. Among these samples, the 7 wt. % Sm^{3+}-doped V_2O_5 composite exhibits the highest specific capacitance. This significant enhancement in capacitance can be attributed to several synergistic effects. First, the incorporation of samarium ions introduces lattice defects and additional electrochemically active sites within the V_2O_5 structure. Second, the presence of reduced graphene oxide improves electrical conductivity and facilitates rapid electron transport throughout the electrode material. Finally, the nanorod morphology provides increased surface area and efficient electrolyte accessibility.

Another important parameter for evaluating supercapacitor performance is cycling stability. The long-term electrochemical stability of the rGO/V_2O_5:Sm^{3+} electrode was examined through repeated CV cycling up to 1000 cycles at a scan rate of 100 mV s^{-1}. The CV curves (Figure 8) recorded during cycling remain almost unchanged in shape, indicating excellent reversibility and electrochemical stability of the electrode material. The ability to maintain stable electrochemical performance during repeated charge–discharge cycles is essential for practical supercapacitor applications.

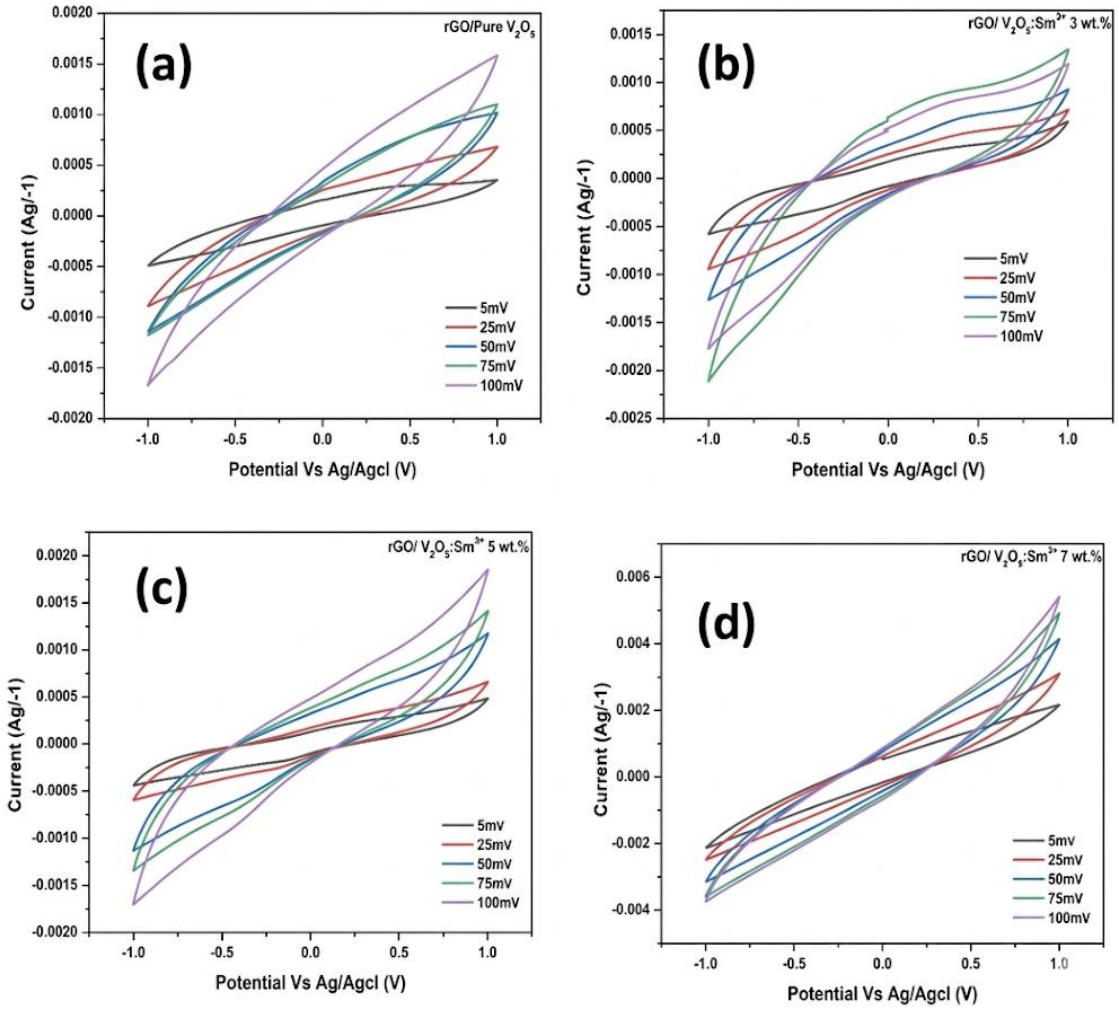

Figure 7. CV of the rGO/V_2O_5:Sm^{3+} (0, 3, 5 and 7 wt. %) nanocomposites at different scan rates (5, 25, 50, 75 and 100 mV s^{-1}).

The observed stability suggests that the composite structure effectively prevents structural degradation and maintains efficient charge transport pathways during prolonged electrochemical operation. Overall, the enhanced electrochemical performance of the rGO/V_2O_5:Sm^{3+} nanocomposites can be attributed to the combined effects of graphene conductivity, rare-earth doping, and nanostructured morphology. These synergistic features significantly improve ion transport, electron mobility, and electrochemical activity within the electrode material, making the synthesized nanocomposite a promising candidate for advanced supercapacitor applications.

3.5 Galvanostatic Charge–Discharge (Gcd) Analysis

The charge–discharge characteristics of the synthesized rGO/V_2O_5 and rGO/V_2O_5:Sm^{3+} (3, 5, and 7 wt.%) nanocomposites were systematically investigated using galvanostatic charge–discharge (GCD) measurements at various current densities ranging from 1 to 5 mA g^{-1} (Figure 9 a–d). The obtained GCD profiles exhibit nonlinear and asymmetric charge–discharge behaviour, which is a clear signature of pseudocapacitive energy storage governed by Faradaic redox reactions associated with the vanadium redox couples (V^{5+}/V^{4+}). Unlike ideal electric double-layer capacitors that display triangular charge–discharge curves, the present electrodes show curved potential–time profiles with a gradual voltage rise during charging and a non-linear decay during discharging. This behaviour confirms that the charge storage mechanism is dominated by diffusion-controlled redox processes rather than purely electrostatic adsorption. The deviation from linearity is particularly pronounced at lower current densities, where electrolyte ions have sufficient time to penetrate deeper into the electrode structure and participate in redox reactions.

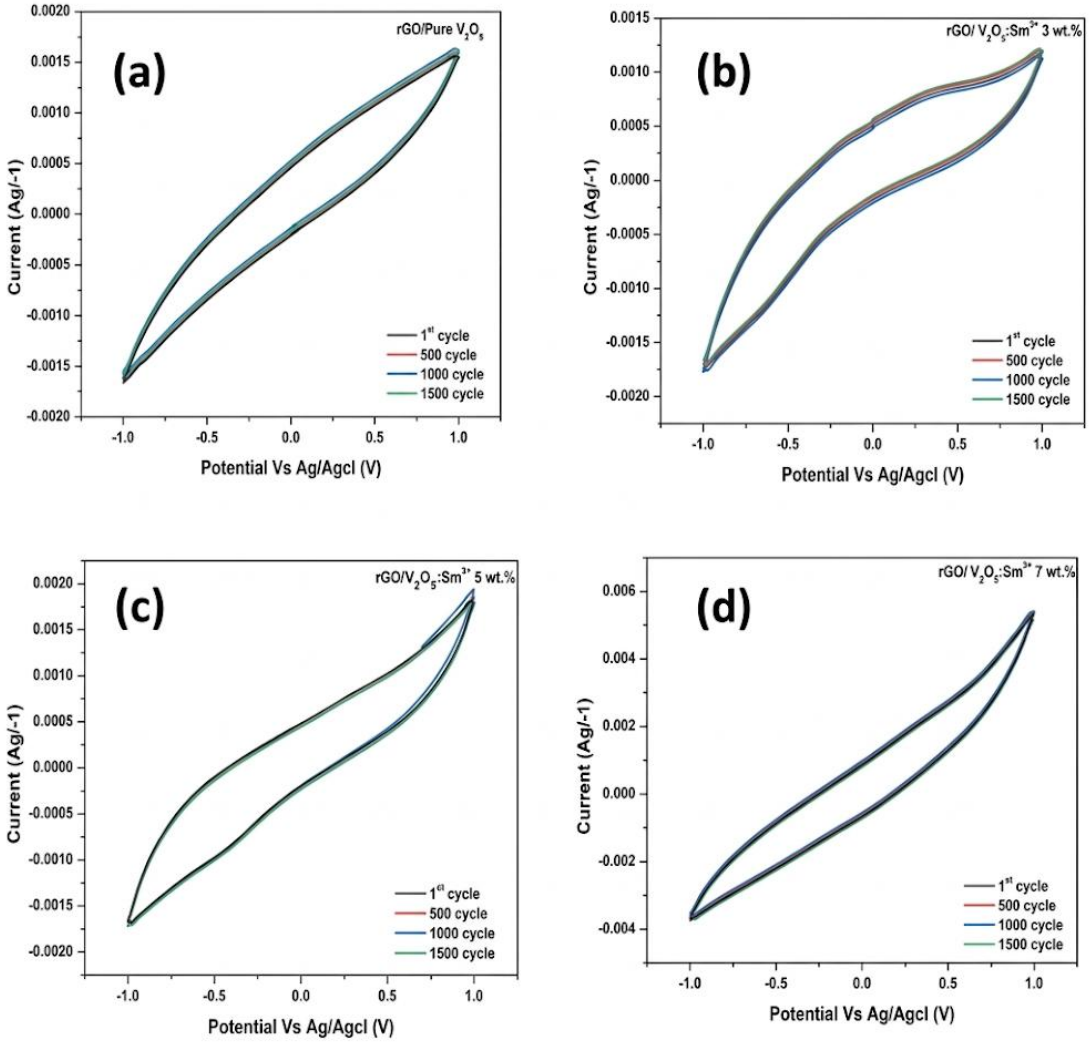

Figure 8. CV curves of rGO/V_2O_5:Sm^{3+} electrode at a scan rate 100 mV s^{-1} upto 1000 cycles.

A notable feature observed in all GCD curves is the presence of a distinct initial potential drop (IR drop) at the beginning of the discharge process. This drop arises from the internal resistance (Rs) of the electrode system, including electrolyte resistance, intrinsic material resistance, and interfacial contact resistance. Importantly, the magnitude of the IR drop decreases with increasing samarium doping concentration, indicating a reduction in internal resistance due to improved electrical conductivity and enhanced charge transport pathways provided by the rGO network and dopant-induced lattice modification. The discharge time, which is directly proportional to the specific capacitance, shows a strong dependence on both current density and samarium content. At a given current density, the discharge duration follows the order rGO/V_2O_5:Sm^{3+} (7 wt. %) > 5 wt. % > 3 wt. % > pure rGO/V_2O_5.

This trend is consistent with the cyclic voltammetry results and confirms that the incorporation of Sm^{3+} ions significantly enhance the charge storage capability of the electrode material. The 7 wt. % doped sample exhibits the longest discharge time, indicating superior capacitance performance. This enhancement can be attributed to several synergistic effects,

1) lattice distortion induced by Sm^{3+} doping, which introduces additional electrochemically active sites,
2) improved electrical conductivity due to the rGO framework, facilitating rapid electron transport, and
3) nanorod morphology of V_2O_5, which provides a high surface area and short ion diffusion pathways.

Furthermore, the GCD curves retain their overall shape across different current densities, indicating good rate capability and structural stability of the electrode materials. Although the discharge time decreases with increasing current density, the

preservation of curve morphology suggests that the electrode maintains efficient charge storage behaviour even under high-rate conditions. The specific capacitance (C_s) of the electrode materials was calculated from the discharge curves using the relation,

$$C_s = \frac{I \cdot \Delta t}{m \cdot \Delta V} \quad (1)$$

Where I is the applied current, Δt is the discharge time, m is the mass of the active material, and ΔV is the potential window excluding the IR drop. The calculated capacitance values are in good agreement with those obtained from cyclic voltammetry, further validating the electrochemical performance of the synthesized nanocomposites. Overall, the GCD analysis demonstrates that samarium doping effectively enhances the electrochemical performance of rGO/V_2O_5 nanocomposites by improving conductivity, increasing active sites, and facilitating ion transport. Among all the samples, the rGO/V_2O_5:Sm^{3+} (7 wt.%) electrode exhibits the best charge–discharge characteristics, confirming its suitability as a high-performance electrode material for advanced supercapacitor applications.

3.6 Electrochemical Impedance Spectroscopy (EIS) Analysis

Electrochemical impedance spectroscopy (EIS) was performed to evaluate the charge transport characteristics and ion diffusion behavior of the rGO/V_2O_5 and rGO/V_2O_5:Sm^{3+} nanocomposite electrodes. The Nyquist plots of all samples (Figure 10) exhibit a predominantly linear response over the entire frequency range, with no clearly distinguishable semicircle in the high-frequency region. This behaviour indicates that the electrochemical process is primarily governed by diffusion-controlled kinetics with negligible charge transfer resistance. The absence of a pronounced semicircle suggests that the charge transfer resistance (Rct) at the electrode–electrolyte interface is very low, which can be attributed to the high electrical conductivity of the rGO network and the effective electronic coupling between V_2O_5 nanorods and graphene sheets. The nearly linear impedance response corresponds to Warburg-type behaviour, arising from the diffusion of electrolyte ions within the porous electrode structure [31].

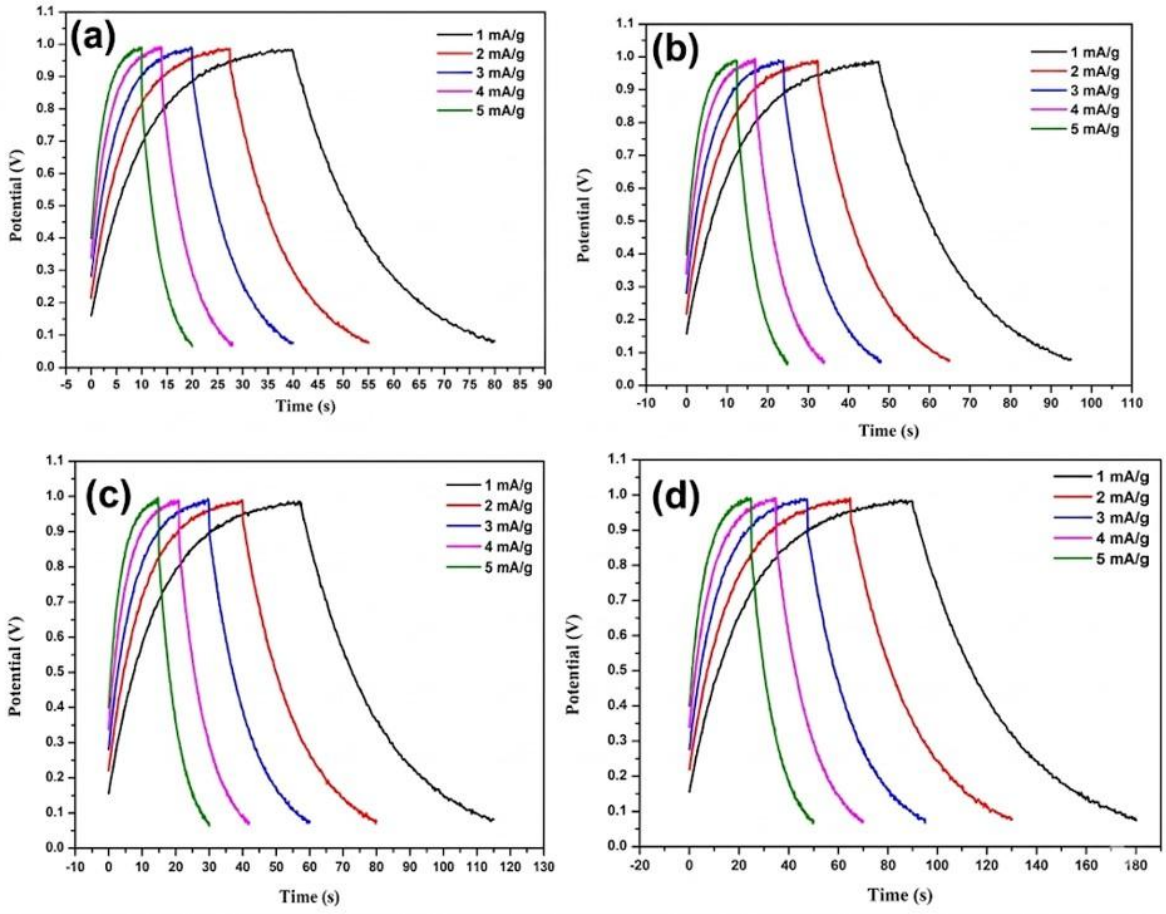

Figure 9. GCD curves of **(a)** rGO/pure V_2O_5 **(b)** rGO/V_2O_5:Sm^{3+} 3 wt. % **(c)** rGO/V_2O_5:Sm^{3+} 5 wt.% **(d)** rGO/V_2O_5:Sm^{3+} 7 wt.% nanocomposites.

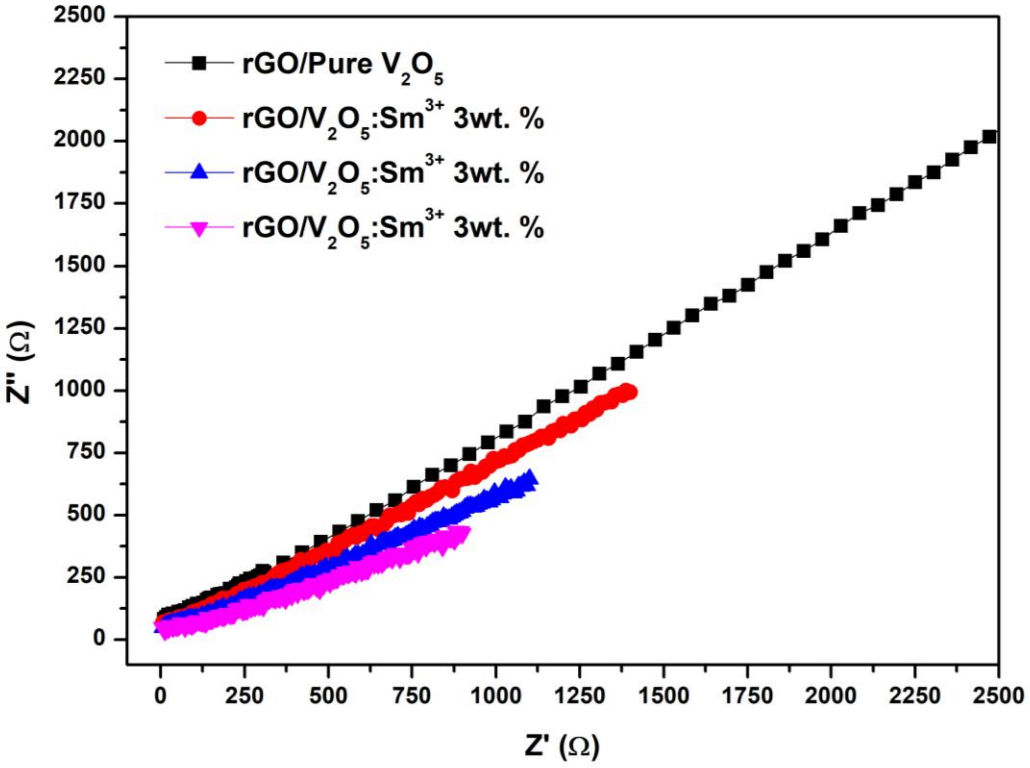

Figure 10. Electrochemical Impedance Spectroscopy

A clear distinction between the samples is observed in terms of the slope and extent of the linear region. The rGO/V_2O_5 (pure) electrode exhibits the longest and steepest line, indicating relatively slower ion diffusion and higher overall impedance. In contrast, the Sm^{3+}-doped samples show progressively reduced impedance values, with the trend, rGO/V_2O_5 (pure) > 3 wt.% > 5 wt.% > 7 wt.%. Among all samples, the rGO/V_2O_5:Sm^{3+} (7 wt.%) nanocomposite displays the shortest and least steep line, suggesting enhanced ion transport kinetics and reduced diffusion resistance. This improvement can be attributed to several synergistic effects. First, the incorporation of samarium ions introduces lattice distortions and defect sites within the V_2O_5 structure, which facilitate ion diffusion and increase electrochemically active sites. Second, the presence of reduced graphene oxide provides a highly conductive network that enhances electron transport throughout the electrode. Third, the nanorod morphology of V_2O_5 offers open channels and short diffusion pathways, enabling efficient electrolyte penetration.

Furthermore, the slight deviation from perfect linearity observed near the low-impedance region indicates a minor contribution from interfacial processes, although it remains insignificant compared to the dominant diffusion-controlled mechanism. The consistent reduction in impedance with increasing samarium content confirms that doping effectively enhances both electronic conductivity and ionic mobility within the electrode material [32]. The EIS results are in strong agreement with the cyclic voltammetry and galvanostatic charge–discharge analyses, where the rGO/V_2O_5:Sm^{3+} (7 wt.%) electrode exhibited the highest specific capacitance and superior rate capability. The combined electrochemical findings demonstrate that samarium doping and graphene hybridization significantly improve charge transport properties, making the nanocomposite an efficient electrode material for high-performance supercapacitor applications.

3.7 Antibacterial Activity

The antibacterial activity of rGO/Pure V_2O_5 and Sm^{3+}-doped rGO/V_2O_5 (7 wt. %) nanocomposites was evaluated against *Escherichia coli* and *Staphylococcus aureus* using the agar well diffusion method at different dosage at the concentration of 1mg/mL (10, 30, and 50 µL). The rGO/Pure V_2O_5 composite exhibited moderate activity against *Escherichia coli*, with zones of inhibition measuring approximately 5 mm, 8 mm, and 15 mm for 10, 30, and 50 µL, respectively. *Staphylococcus aureus*, showing inhibition zones of 4 mm and 5 mm at lower concentrations and a maximum zone of 25 mm at 50-µL dosage.

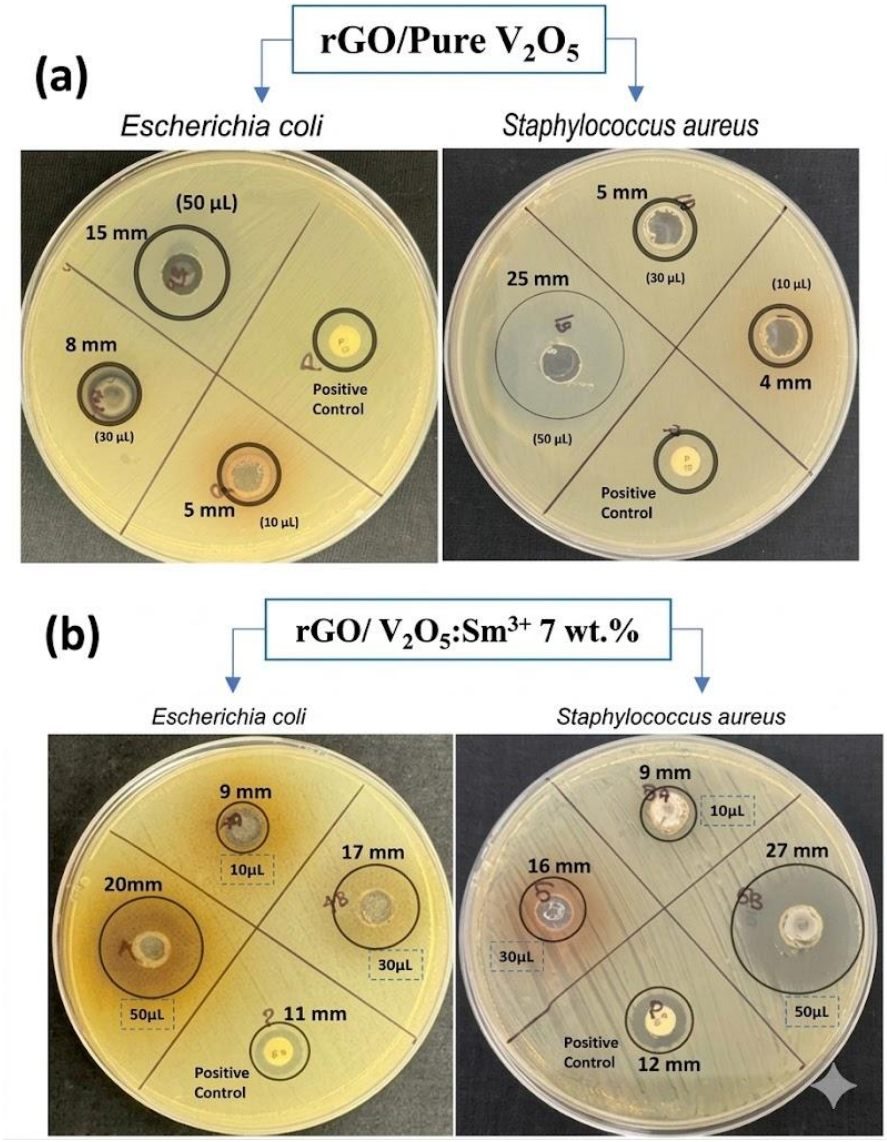

Figure 11. Antibacterial activity of (a) rGO/Pure V_2O and (b) Sm^{3+}-doped rGO/V_2O_5 against human pathogenic bacteria

The Sm^{3+}-doped rGO/V_2O_5 (7 wt.%) nanocomposite demonstrated significantly enhanced antibacterial efficacy against both bacterial strains, with inhibition zones of 9 mm, 17 mm, and 20 mm for *Escherichia coli* and 9 mm, 16 mm, and 27 mm for *Staphylococcus aureus* at 10, 30, and 50 µL, respectively. The positive control exhibited consistent and distinct inhibition zones, confirming the reliability of the experimental conditions. Overall, the results indicate that Sm^{3+} doping substantially improves the antibacterial performance of the rGO/V_2O_5 nanocomposite against both Gram-negative and Gram-positive bacteria, on the dosage depended manner (Figure 11).

The presence of reduced graphene oxide (rGO) plays a crucial role in enhancing antibacterial performance by acting as an electron acceptor and transporter, thereby suppressing charge recombination and amplifying ROS production [15,17]. The large surface area of rGO also promotes strong physical interactions with bacterial cell walls, facilitating close contact between the nanocomposite and microbial cells. This interaction can lead to mechanical stress and direct membrane damage, resulting in increased permeability, leakage of intracellular components, and eventual cell death [16, 33]**.** The enhanced antibacterial activity observed for the Sm^{3+}-doped rGO/V_2O_5 (7 wt.%) nanocomposite against *Escherichia coli* and *Staphylococcus aureus* can be attributed to synergistic effect and interactions of nanocomposite and the bacterial cell membrane, which leads the potential antibacterial activity against test pathogens [20, 14]. In the present study indicates the dose dependent antibacterial activity suggests that increased nanocomposite dosage enhances ROS accumulation

and intensifies membrane disruption effects. Overall, the maximum activity of the Sm^{3+}-doped rGO/V_2O_5 nanocomposite is attributed to a combined mechanism involving oxidative stress mediated by ROS, efficient charge separation facilitated by rGO, and direct physical damage to bacterial membranes, making it a promising candidate for biomedical and cosmeceutical applications.

5. Conclusion and Future Perspectives

In this study, rGO/V_2O_5 and samarium-doped rGO/V_2O_5:Sm^{3+} nanocomposites with different dopant concentrations were successfully synthesized using a simple co-precipitation method followed by thermal treatment. Structural characterization using X-ray diffraction confirmed the formation of orthorhombic V_2O_5 with good crystallinity and phase purity. The calculated crystallite sizes ranged between approximately 66 nm and 87 nm, indicating nanoscale structural features that are beneficial for electrochemical applications. Slight variations in lattice parameters and microstrain values were observed with increasing Sm^{3+} doping concentration, suggesting that samarium ions were successfully incorporated into the V_2O_5 lattice. Morphological investigations using SEM and HR-TEM revealed that the synthesized nanocomposites possess a rod-like nanostructure distributed over reduced graphene oxide sheets. The formation of this hybrid architecture provides a conductive network that enhances electron transport while also preventing nanoparticle aggregation. Energy dispersive spectroscopy further confirmed the presence of vanadium, oxygen, samarium, and carbon elements with uniform distribution throughout the composite structure.

Electrochemical studies carried out using cyclic voltammetry demonstrated clear pseudocapacitive behaviour associated with reversible Faradaic redox reactions. Among the prepared samples, the rGO/V_2O_5:Sm^{3+} nanocomposite containing 7 wt.% samarium exhibited the highest specific capacitance of approximately 386.70 F g^{-1}. This enhanced performance is attributed to the combined effects of graphene-assisted electrical conductivity, rare-earth-induced lattice modification, and the nanorod morphology of V_2O_5. The electrode material also displayed good electrochemical stability during repeated cycling, indicating its suitability for practical supercapacitor applications. The results obtained in this work demonstrate that rare-earth doping combined with graphene hybridization is an effective strategy for improving the electrochemical performance of transition metal oxide electrodes. The rGO/V_2O_5:Sm^{3+} nanocomposite developed in this study shows promising characteristics for use in next-generation energy storage devices, particularly in high-power supercapacitor systems. Future research could further improve the performance of such nanocomposite electrodes by optimizing synthesis parameters, exploring other rare-earth dopants, and investigating different graphene loading ratios. In addition, advanced electrochemical analyses such as galvanostatic charge–discharge measurements, electrochemical impedance spectroscopy, and long-term cycling tests would provide deeper insight into the charge storage mechanism and stability of these materials. Such studies would contribute to the development of more efficient and durable electrode materials for sustainable energy storage technologies. The Sm^{3+}-doped rGO/V_2O_5 (7 wt. %) nanocomposite showed a much stronger antibacterial effect against both bacterial strains. At 50 µL, the inhibition zones were 20 mm for Escherichia coli and 27 mm for Staphylococcus aureus. The positive control showed clear and consistent inhibition zones, which proved that the experimental conditions were reliable. In general, the results show that Sm^{3+} doping greatly improves the antibacterial activity of the rGO/V_2O_5 nanocomposite against both Gram-negative and Gram-positive bacteria, depending on the dose. The highest activity of the Sm^{3+}-doped rGO/V_2O_5 nanocomposite is due to a combination of oxidative stress caused by ROS, efficient charge separation caused by rGO, and direct physical damage to bacterial membranes. This makes it a good candidate for use in medicine and cosmetics.

References

[1] G. Ramkumar, S. Kannan, V. Mohanavel, S. Karthikeyan, A. Titus, The Future of Green Mobility: A Review Exploring Renewable Energy Systems Integration in Electric Vehicles. Results in Engineering, 27, (2025) 105647. https://doi.org/10.1016/j.rineng.2025.105647

[2] N.A. Wadodkar, R.S. Salunke, S.K. Pawar, A. Umar, A.A. Ibrahim, S. Akbar, S.A. Ansari, S. Baskoutas, D.J. Shirale, Next-Generation Supercapacitors: Advances in Binder-Free Electrodes, Scalable Fabrication, and Emerging Applications. Advanced Sustainable Systems, 10(1), (2025). https://doi.org/10.1002/adsu.202500599

[3] H. Gamal, A.M. Elshahawy, S.S. Medany, M.A. Hefnawy, M. Shalaby, Recent Advances of Vanadium Oxides and their Derivatives in Supercapacitor Applications: A Comprehensive Review. Journal of Energy Storage, 76, (2023) 109788.https://doi.org/10.1016/j.est.2023.109788

[4] Y. Wei, K.D. Kumar, L. Zhang, J. Li, Pseudocapacitive Materials for Energy Storage: Properties, Mechanisms, and Applications in Supercapacitors and Batteries. Frontiers in Chemistry, 13, (2025) 1636683. https://doi.org/10.3389/fchem.2025.1636683

[5] B.B. Patowary, D. Brahma, A. Mondal, Study of RuO_2- and MnO_2-based Electrode Materials and their Performance Review in Conjunction with Pani for Supercapacitor Applications. Ionics, 31(1), (2024) 67–115. https://doi.org/10.1007/s11581-024-05828-3

[6] C.C. Ganesh, B.R. Krushna, I. Pruthviraj, G. Ramakrishna, S. Sharma, A. George, S. Mishra, U. Premkumar, K. Manjunatha, S.Y. Wu, H. Kuo, V. Shivakumar, S. Devaraja, H. Nagabhushana, Green Synthesis of Ce3+ doped V_2O_5 NPs as an Advanced Electrode Material for Possible Supercapacitor and Therapeutic Applications. Journal of the Taiwan Institute of Chemical Engineers, 174, (2025) 106223.https://doi.org/10.1016/j.jtice.2025.106223

[7] A. Vedpathak, M. Desai, B. Thombare, R.S. Kalubarme, G. Guan, S. Bhagwat, S.D. Sartale, Evolution of α-V_2O_5 into Electrochemically Transformed Nav_3o_8 Structure: Structural Changes and Supercapacitor Application. Journal of Electroanalytical Chemistry, 958, (2024)118150.https://doi.org/10.1016/j.jelechem.2024.118150

[8] A. Viswanathan, B. Prakashaiah, V. Subburaj, A.N. Shetty, High Energy Reduced Graphene Oxide/Vanadium Pentoxide/Polyaniline Hybrid Supercapacitor for Power Backup and Switched Capacitor Converters. Journal of Colloid and Interface Science, 545, (2019) 82–93. https://doi.org/10.1016/j.jcis.2019.03.013

[9] F.A. Ibrahim, Electrical Conductivity Enhancement of V_2O_5–P_2O_5–Bi_2O_3 Glasses by Nanocrystallization. Journal of Electronic Materials, 51(2), (2021) 621–625. https://doi.org/10.1007/s11664-021-09308-6

[10] R. Yadav, A.K. Chadar, S. Sardar, S. Singh, P. Kushwaha, S.P. Singh, V_2O_5 Nanorods and V2O5-rGO Composite: Achieving High Specific Capacitance through Nanostructuring and Synergistic Interactions. Materials Science and Engineering B, 313, (2024) 117926. https://doi.org/10.1016/j.mseb.2024.117926

[11] A.G. Adugna, A.A. Assegie, M.A. Alemu, Systematic Optimization of High-Throughput Microwave-Assisted Hydrothermal Synthesis of Reduced Graphene Oxide for Electrochemical Energy Storage Applications. Carbon Trends, 21, (2025) 100581. https://doi.org/10.1016/j.cartre.2025.100581

[12] N.A. Niaz, S. Naz, A.S. Khan, F. Hussain, M. Kanwal, A. Arooj, S. Ahmad, D. Ozer, M. Tariq, A.M. Tighezza, Synthesis and Characterization of V_2O_5/RGO Hybrid Nanowire Composites as Electrode Materials for Energy Storage Applications. Journal of Inorganic and Organometallic Polymers and Materials, (2025). https://doi.org/10.1007/s10904-025-03994-z

[13] G.P. Pandey, T. Liu, E. Brown, Y. Yang, Y. Li, X.S. Sun, Y. Fang, J. Li, Mesoporous Hybrids of Reduced Graphene Oxide and Vanadium Pentoxide for Enhanced Performance in Lithium-Ion Batteries and Electrochemical Capacitors. ACS Applied Materials & Interfaces, 8(14), (2016) 9200–9210. https://doi.org/10.1021/acsami.6b02372

[14] C.C. Ganesh, B.R. Krushna, N. Navya, S. Sharma, V. Vickneshwaran, K. Thangamani, S. Mohapatra, S. Ray, K. Manjunatha, S.Y. Wu, S. Yu, J.K. Galivarapu, G. Ramakrishna, R. Arunakumar, H. Nagabhushana, B.A. Al-Asbahi, Sustainable synthesis of V_2O_5:Sm^{3+} Nanoparticles for Malachite Green Photodegradation and High-Efficiency Supercapacitors. Journal of the Taiwan Institute of Chemical Engineers, 178, (2025) 106341. https://doi.org/10.1016/j.jtice.2025.106341

[15] X. Zhou, M. Zhou, S. Ye, Y. Xu, S. Zhou, Q. Cai, G. Xie, L. Huang, L. Zheng, Y. Li, Antibacterial Activity and Mechanism of the Graphene Oxide (Rgo)-Modified Tio_2 Catalyst Against Enterobacter hormaechei. International Biodeterioration & Biodegradation, 162, (2021) 105260.https://doi.org/10.1016/j.ibiod.2021.105260

[16] R. Mann, D. Mitsidis, Z. Xie, O. McNeilly, Y.H. Ng, R. Amal, C. Gunawan, Antibacterial Activity of Reduced Graphene Oxide. Journal of Nanomaterials, 2021(1), (2021) 9941577. https://doi.org/10.1155/2021/9941577

[17] R. Chaudhary, N.B. Singh, G. Nagpal, F.K, Saah, Antibacterial Activity of Reduced Graphene-Silver Oxide Nanocomposite against Gram-Negative Bacteria. The Microbe, 5, (2024)100221.https://doi.org/10.1016/j.microb.2024.100221

[18] H. Mohan, V. Ramalingam, J.M. Lim, S.W. Lee, J. Kim, J.H. Lee, Y.J. Park, K.K. Seralathan, B.T. Oh, E-waste based Graphene Oxide/V_2O_5/Pt Ternary Composite: Enhanced Visible Light Driven Photocatalyst for Anti-Microbial and Anti-Cancer Activity. Colloids and Surfaces A: Physicochemical and Engineering Aspects, 607, (2020) 125469. https://doi.org/10.1016/j.colsurfa.2020.125469

[19] H. Chaudhary, K. Chaudhary, S. Zulfiqar, M.S. Saif, I.A. Alsafari, I. Shakir, P.O. Agboola, M. Safdar, M.F., Warsi, Fabrication of Reduced Graphene Oxide Supported Gd^{3+} Doped V_2O_5 Nanorod Arrays for Superior Photocatalytic and Antibacterial Activities. Ceramics International, 47(23), (2021) 32521-32533. https://doi.org/10.1016/j.ceramint.2021.08.146

[20] S. Cha, J.Y. Chung, S. Yang, S.C. Lee, C.W. Lee, C.W.L. Cheng, J.B. Kim, N.J. Kim, A. Park, H. Choi, J. Sinn, Biocompatible but Antibacterial Mechanism of Graphene Oxide for Sustainable Antibiotics. Advanced Functional Materials, (2026) e74695. https://doi.org/10.1002/adfm.74695

[21] S. Hu, B. Wang, M. Zhu, Y. Ma, Z. Lv, H. Wang, High-Performance 1D Type-II Tio_2@Zno Core-Shell Nanorods Arrays Photoanodes for Photoelectrochemical Solar Fuel Production. Applied Surface Science, 403, (2017) 126–132. https://doi.org/10.1016/j.apsusc.2017.01.093

[22] S. Nandakumar, D.A. Nayana, N.S. George, S.P. Nair, S. Athira, L.M. Jose, A. Joseph, J. Alex, P.K. Manoj, D. Sajan, Co-Precipitated V2O5 Nanoparticles for Supercapacitor and Photocatalytic Applications. Journal of Materials Science: Materials in Electronics, 36(34), (2025). https://doi.org/10.1007/s10854-025-16236-2

[23] S.A. Bhat, A.M. Tantray, J.U. Ahsan, M. Ikram, Exploring the Supercapacitive Potential of Sm^{3+} Doped $Cofe_2o_4$ Nanoparticles: Enhanced Magnetic and Dielectric Properties. Ceramics International, 50(14), (2024) 26220–26233. https://doi.org/10.1016/j.ceramint.2024.04.362

[24] R. Kumar, D.S. Saini, A. Soam, Reduced Graphene Oxide Modified with Bismuth Iron Oxide Nanoparticles for Supercapacitor Application. Discover Applied Sciences, 7(11), (2025). https://doi.org/10.1007/s42452-025-07887-1

[25] D. Govindarajan, V.U. Shankar, R. Gopalakrishnan, Supercapacitor Behavior and Characterization of RGO Anchored V_2O_5 Nanorods. Journal of Materials Science: Materials in Electronics, 30(17), (2019) 16142–16155. https://doi.org/10.1007/s10854-019-01984-9

[26] J.A. Rafi, R. Kumar, W.K. Tan, G. Kawamura, A. Matsuda, $BiVO_4$-Graphene Nanocomposites: Recent Progress toward Photocatalytic Environmental Remediation of Pollutants. Journal of Environmental Chemical Engineering, (2026) 122107. https://doi.org/10.1016/j.jece.2026.122107

[27] R. Baddour-Hadjean, M.S. Renard, N. Emery, L. Huynh, M. Le, J. Pereira-Ramos, The Richness of V_2O_5 Polymorphs as Superior Cathode Materials for Sodium Insertion. Electrochimica Acta, 270, (2018) 129–137. https://doi.org/10.1016/j.electacta.2018.03.062

[28] W. Myint, K. Lolupiman, C. Yang, P. Woottapanit, W. Limphirat, P. Kidkhunthod, M. Muzakir, M. Karnan, X. Zhang, J. Qin, Exploring The Electrochemical Superiority of V_2O_5/Tio_2@Ti_3C_2-Mxene Hybrid Nanostructures for Enhanced Lithium-Ion Battery Performance. ACS Applied Materials & Interfaces, 16(40), (2024) 53764–53774. https://doi.org/10.1021/acsami.4c10656

[29] A. Raza, K. Shehzad, A. Shehzad, F. Rasheed, A. Ahmed, S. Ali, N. Li, M. Hussain, K.I. Anojaidi, W.A. Alsuwaylih, M.A. Alsuwaylih, A.H. Almubarak, S. Wang, Z. Wang, Rational Design of Graphene-Metal Oxide Nanocomposites for Advanced Supercapacitors: Synergistic Mechanisms, Sustainable Synthesis, and Scalability Challenges. Results in Engineering, 29, (2026) 109368. https://doi.org/10.1016/j.rineng.2026.109368

[30] D. Ma, C. Han, B. Liu, J. Chen, M. Wu, D. Guan, Vanadium Oxide-Based Electrode Materials for Advanced Supercapacitors: A review. Energy & Fuels, 38(12), (2024) 10494–10516.https://doi.org/10.1021/acs.energyfuels.4c00725

[31] S.D. Xu, Q.C. Zhuang, L.L. Tian, Y.P. Qin, L. Fang, S.G. Sun, Impedance Spectra of Nonhomogeneous, Multilayered Porous Composite Graphite Electrodes for Li-Ion Batteries: Experimental and Theoretical Studies. The Journal of Physical Chemistry C, 115(18), (2011) 9210-9219. https://doi.org/10.1021/jp107406s

[32] M.B. Askari, and P. Salarizadeh, State-of-the-art Review on Reduced Graphene Oxide for Supercapacitor Electrode Applications. Results in Engineering, (2025) 107429. https://doi.org/10.1016/j.rineng.2025.107429

[33] A. Darmawan, A. Pratiwi, M. Al Fahmi, H. Muhtar, R.M. Tsuraya, Y. Astuti, Antibacterial Activity of Graphene Oxide/Zno/Salicylic Acid Composite Against Gram-Negative and Gram-Positive Bacteria. Materials Chemistry and Physics, 343, (2025) 131020. https://doi.org/10.1016/j.matchemphys.2025.131020

Author Contribution Statement

Senthil Kumar Nagarajan: Conceptualization. Methodology, Investigation, Validation, Analaysis. S. Akshaya Devi: Methodology. S. Aarthi: Methodology, R. Swathi: Methodology. S. Nagasundar: Data curation. T. Kannan: Data curation. M. Gowtham - Data Curation, Writing, review and editing. All the authors read and approved the final version of the manuscript.

Data Availability Statement

Data will be a made available on request from corresponding author non reasonable request.

Does this article screened for similarity?

Yes

Acknowledgement

One of the authors Dr. Senthil Kumar Nagarajan gratefully acknowledges the Tamil Nadu State Council for Science and Technology for awarding the Student Project Scheme.

Conflict of interest

The Author's declares that there is no conflict of interest anywhere.

About the License